

# Reprint

## **Far-End Crosstalk Identification Method Based on Channel Training Sequences**

*N. Papandreou and Th. Antonakopoulos*

IEEE Transactions on Instrumentation and Measurement

---

VOL. 54 NO. 6, DECEMBER 2005, pp. 2204-2212

---

**Copyright Notice:** This material is presented to ensure timely dissemination of scholarly and technical work. Copyright and all rights therein are retained by authors or by other copyright holders. All persons copying this information are expected to adhere to the terms and constraints invoked by each author's copyright. In most cases, these works may not be reposted or mass reproduced without the explicit permission of the copyright holder.

# Far-End Crosstalk Identification Method Based on Channel Training Sequences

Nikolaos Papandreou, *Member, IEEE*, and Theodore Antonakopoulos, *Senior Member, IEEE*

**Abstract**—Far-end crosstalk identification results to improved frequency spectrum utilization in asymmetric digital subscriber line (ADSL) systems. The accurate determination of the crosstalk coupling function is a demanding task that is affected by various system impairments. In this paper, we present a new real-time method that exploits the exchange of signaling information between the modems of a new activated ADSL line in order to determine the crosstalk function between this line and any other active line in the binder. Each remote modem subtracts the decoded data from the received signal, decreases the noise effect of the previously identified crosstalkers, is synchronized to the disturber's timing and then applies a least-squares estimator for identifying the new crosstalk coupling function. The method is used along with a maximum margin bit-loading algorithm in order to provide the best possible estimation results. The estimated crosstalk coupling functions, the transfer function of each line and the noise measurements can be exploited by a centralized bit-loading algorithm for maximizing the total system performance in terms of maximum achievable data rate and/or bit error rate.

**Index Terms**—Centralized bit-loading, crosstalk, digital subscriber line, identification, noise, signaling protocol.

## I. INTRODUCTION

**D**IGITAL subscriber lines (DSL) technology provides high-speed data communication services to end-users utilizing the existing twisted-pair infrastructure. The achievable data rate at a DSL link depends on the characteristics of the loop environment in terms of line attenuation and noise level. Crosstalk interference induced by adjacent lines is one of the largest noise impairments that reduce the performance of services operating in the same binder [1]. As the support of more DSL services is required, the need for controlling the total interference becomes a critical issue. Spectrum management of DSL technologies refers to guidelines that minimize the potential of crosstalk interference and maximize the frequency spectrum utilization in multipair loop cables [2]. However as the demand for higher speed services increases and the number of DSL users continues to grow, the development of methods for achieving coordination among various DSL modems in order to improve the

total binder performance has become an appealing challenge. Dynamic spectrum management aims to the development of crosstalk identification methods that enhance the spectrum management value [3]–[5].

Crosstalk identification in DSL systems has attracted a lot of attention due to the significant benefits of having an accurate description of all cable services that generate crosstalk into a given pair. A non modem-based approach is presented in [6]. The crosstalk sources are identified in the frequency domain by finding the maximum correlation with a “basis set” of representative measured crosstalk coupling functions. The “basis set” is generated by multiplying the canonical set of measured pair-to-pair crosstalk coupling functions with the power spectral density (PSD) of each specific type of DSL. However the concept of the “basis set” applies only to near-end crosstalk (NEXT), where the “basis set” depends only on the disturber's technology.

The idea of an impartial third party that identifies the crosstalk coupling functions among the twisted pairs of a binder is described in [7]. A third party site collects the transmitted and received signals from all modems in the binder during a given time span. Initially, a cross-correlation technique is applied, in order to estimate the timing differences between the signals from different providers in the same bundle. Next, a least-squares method is used for estimating the crosstalk coupling functions and for finer scaling of the timing-offset among different operators.

In this paper, we present a far-end crosstalk (FEXT) identification method for asymmetric digital subscriber line (ADSL) systems operating in the same binder [8]. The method is based on measurements performed at each active modem, when a new line is activated and channel training is performed. Each active modem removes the decoded data from the received data stream and estimates the new crosstalk coupling function by being synchronized at the disturber's timing. The estimated crosstalk coupling functions are collected in a management unit at the central office (CO) in order to create a local database that contains the crosstalk coupling functions between any pair of DSL lines, irrespective to the order of activation. The CO coordinates the various signaling protocols and re-initializes the modems, when it is necessary. The information of the crosstalk database can be used by the CO and the various modems in order to achieve better system performance in terms of optimum bit and power loading, improved data rate and/or less bit error rate.

Section II presents the basic aspects of the FEXT environment of an ADSL binder and describes the bit-loading algorithm used to achieve maximum noise margin. Section III describes the process for extracting the crosstalk-related information in a

Manuscript received October 30, 2003; revised April 28, 2005. This work was supported in part by the “Karatheodoris” Research and Development Program of the University of Patras, Greece, and in part by Project 00BE33 entitled “Digital Subscriber Lines Technology” of the Greek Ministry of Industry.

N. Papandreou is with the Department of Electrical Engineering and Computers Technology, University of Patras, 26500 Rio-Patras, Greece, and also with the Research Academic Computer Technology Institute, 26100 Patras, Greece (e-mail: npapandr@cti.gr).

T. Antonakopoulos is with the Department of Electrical Engineering and Computers Technology, University of Patras, 26500 Rio-Patras, Greece (e-mail: antonako@upatras.gr).

Digital Object Identifier 10.1109/TIM.2005.858578

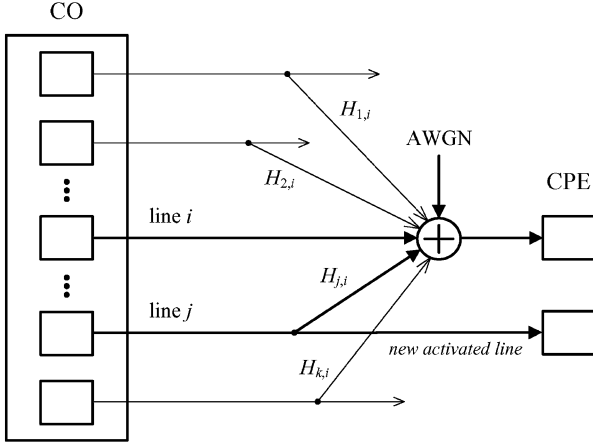


Fig. 1. FEXT crosstalk environment for FDM downstream ADSL transceivers.

disturbed line and how the disturbed modem is synchronized to the disturber's timing. Section IV presents the method used for identifying the crosstalk coupling function and discusses the effect of various system parameters on the crosstalk identification method. Finally, Section V describes how the crosstalk identification procedure can be used in a binder in order to determine the crosstalk coupling function between any pair of DSL lines.

## II. POWER ALLOCATION, FEXT, AND NOISE MARGIN

Frequency division multiplexing (FDM) is used to avoid self-NEXT in ADSL systems [9]. Fig. 1 shows an indicative FEXT interference environment, based on a number of downstream ADSL links, i.e., from CO to the customer premises equipment (CPE). Given that  $k - 1$  lines are already operational, we aim to determine a crosstalk identification mechanism at the CPE receiver of line  $i$ , when a new line  $j$ , considered as the *disturber*, is activated.

When the first line in a binder is activated, it experiences only additive white Gaussian noise (AWGN), while all other lines experience AWGN and FEXT noise during initialization. If the crosstalk coupling functions are not known, the receivers treat the total noise as Gaussian in order to calculate the bit-loading distributions. However, if the crosstalk coupling functions, the bit allocation and the power profile used on the active lines are known, different bit-loading distributions can be specified that result to better system performance [10].

### A. Maximum Margin Loading Algorithm

When there are multiple active lines in the same binder, the introduced crosstalk noise is the dominant noise in the system. The best performance, in terms of noise tolerance, is achieved when a bit-loading mechanism is used that achieves the maximum possible noise margin for a given data rate.

In this section, we present an algorithm for determining the transmit power and the number of bits allocated at each ADSL subchannel. ADSL technology uses the discrete multitone (DMT) transmission method that decomposes the channel spectrum into a set of  $N/2 = 256$  narrow-band subchannels [11]. The loading algorithm aims in the maximization of the system performance margin  $\gamma_m$ , given a target rate  $B_{\text{target}}$ ,

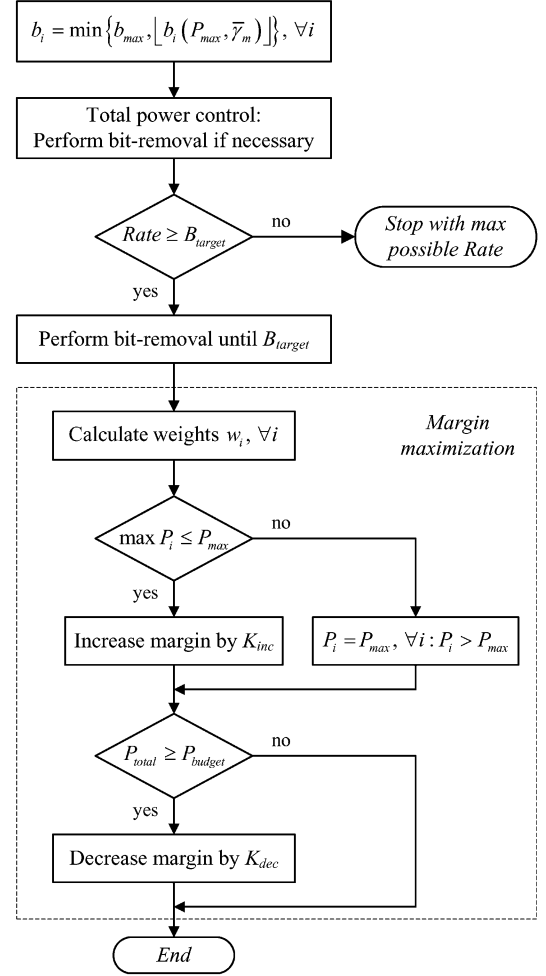


Fig. 2. Maximum margin bit-loading algorithm (for constant margin  $w_i = 1, \forall i$ ).

a power budget  $P_{\text{budget}}$  and a transmit PSD mask. Since the system margin reflects the amount of channel-to-noise ratio degradation that the system can tolerate, while still operating under the desired bit error rate, the margin maximization problem is equivalent to the power minimization problem with zero margin and final gain scaling so as to utilize the available power budget [12].

The proposed algorithm takes advantage of the bit-removal scheme [13], in order to obtain the bit distribution for the target data rate under minimum power. We also consider a minimum margin that our system should achieve. The loading procedure, shown in Fig. 2, is as follows.

- 1) Use a minimum system margin  $\bar{\gamma}_m$  and fill each sub-channel with the lesser of the following limits: maximum allowable number of bits  $b_{\text{max}}$  in a subchannel and number of bits corresponding to the maximum power  $P_{\text{max}}$  imposed by the PSD mask.
- 2) Round the bits in all subchannels to  $\lfloor b_i \rfloor$ , where  $i = 1, \dots, N/2$ , so that the peak power constraint is not violated, and adjust the power in each subchannel based on the new integer bit distribution.
- 3) Calculate the power over all subchannels. If the total power is greater than the power budget, then remove the

most power-expensive bits in order to meet the power budget constraint.

- 4) Sum the bits in all subchannels. If the total rate is less than the target rate, then stop and indicate maximum possible rate with minimum margin, otherwise remove the most power-expensive bits [13] in order to meet the target rate and calculate the power over all subchannels  $P_{\text{total}}$ .
- 5) Margin maximization can be achieved by using one of the following two strategies: *constant margin* for all subchannels and *variable margin* based on a weighted subchannel allocation profile.
  - *Constant Margin*: Determine the maximum subchannel power,  $\max P_i$ . Under the PSD mask and power budget constraints, the additional system margin  $\hat{\gamma}_{m,i}$  (in dB) for all used subchannels is given by the lesser of the following ratios:  $10 \cdot \log_{10}(P_{\text{budget}}/P_{\text{total}})$  and  $10 \cdot \log_{10}(P_{\text{max}}/\max P_i)$ ,  $\forall i = 1, \dots, N/2$ .
  - *Variable Margin*: The final margin distribution reflects the impact of FEXT over the ADSL bandwidth, so that more margin is provided to subchannels that are subject to stronger crosstalk. If we denote as  $w_i$  the weight for subchannel  $i$ , the additional margin in each subchannel is  $10 \cdot \log_{10}(w_i)$ . More details are given at the end of this section.
- 6) Scale the power over all subchannels with the additional margin  $\hat{\gamma}_{m,i}$ , in order to obtain the final power distribution. The total margin (in decibels) for subchannel  $i$  is given by  $\gamma_{m,i} = \bar{\gamma}_m + \hat{\gamma}_{m,i}$ .

As indicated, the weighted margin maximization strategy aims in a margin distribution that takes into account the PSD of FEXT noise over the ADSL bandwidth. Equation (1) describes the FEXT noise model, generated by  $N_d$  crosstalk disturbers of the same type, where  $S(f)$  is the PSD of the disturbing signal,  $H(f)$  is the transfer function of the loop,  $l$  is the coupling path length in feet,  $f$  is the frequency in hertz, and  $K_F = 7.74 \cdot 10^{-21}$  is a constant determined by measurements [2]

$$\text{Fext}(f) = S(f) \cdot |H(f)|^2 \cdot l \cdot K_F \cdot N_d^{0.6} \cdot f^2. \quad (1)$$

From the above model, it is evident that the FEXT noise spectrum is proportional to the square of the frequency, but also exhibits attenuation as the frequency increases due to the loop transfer function term. Although this model is quite pessimistic (it expresses the 1% worst case crosstalk), it can be used in order to shape the margin weights. In particular, if  $\gamma_{m,i} = w_i \bar{\gamma}_m$  is the weighted margin distribution for a given system noise and FEXT crosstalk is induced, we want to degrade the margin distribution to a minimum value for all subchannels. In this case

$$w_i \bar{\gamma}_m = (1 + F_i/U_i) \bar{\gamma}_{m,c} \quad (2)$$

where  $U_i$  is the current system noise,  $F_i$  is the anticipated injected FEXT, and  $\bar{\gamma}_{m,c}$  is a constant value that our system should maintain. We choose  $\bar{\gamma}_{m,c} = c \bar{\gamma}_m$  ( $0 \leq c \leq 1$ ) and we use (1)

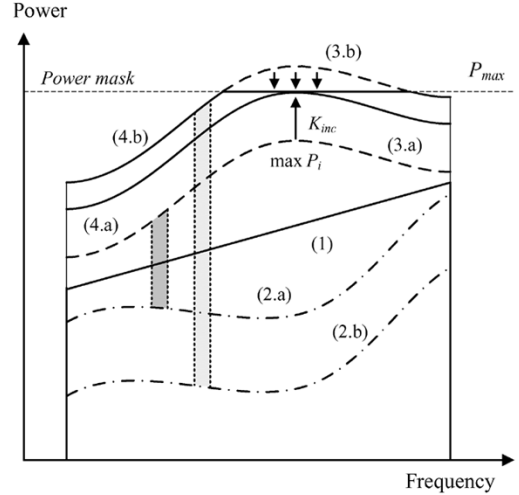


Fig. 3. Example of a weighted margin distribution.

to model the FEXT interference. Then the weights distribution is given by

$$w_i = c \left( 1 + \frac{S_i \cdot |H_i|^2 \cdot l \cdot K_F \cdot ((N_{\text{total}} - 1)^{0.6} - N_{\text{act}}^{0.6}) \cdot f_i^2}{U_i} \right) \quad (3)$$

where  $N_{\text{total}}$  is the total number of lines in the binder and  $N_{\text{act}}$  is the number of lines that are already active (not including the line under initialization). Note that in the above equation the noise  $U_i$  and loop transfer function coefficient  $H_i$  in subchannel  $i$  were estimated during channel training. In order to determine the disturbing signal  $S_i$ , a realistic assumption is that a similar power allocation mechanism is used at all lines.

The final weighted margin distribution can be described by the example of Fig. 3. Let curve 1 be the minimum margin power distribution of step 4) in the previously described loading process. Curves 2.a and 2.b represent two cases of margin degradation due to FEXT noise from  $N_d$  disturbing lines, that are active in the binder. Using (3), we calculate an initial weighted margin distribution  $w_i \bar{\gamma}_m$ , that reflects the FEXT spectrum. We distinguish two cases for the resulting power distribution: the distribution lies below the maximum power mask for all used subchannels (curve 3.a) or some of the subchannels exceed the power constraint (curve 3.b). In the first case, we determine the maximum power  $\max P_i$  over all subchannels and we further increase the margin by  $K_{\text{inc}} = P_{\text{max}}/\max P_i$  (curve 4.a). In the second case, we decrease to  $P_{\text{max}}$  all subchannels that exceed the power constraint (curve 4.b). Then, in both cases total power control is performed. We calculate the power  $P_{\text{total}}$  over all subchannels. If total power is greater than the power budget, we decrease all margins uniformly by  $K_{\text{dec}} = P_{\text{total}}/P_{\text{budget}}$ .

### B. Signaling and FEXT Noise

When a new line is activated, various initialization procedures are performed [9] and the CPE receiver estimates the transfer function and noise power in the downstream link. The signaling protocol of DSL systems defines the procedures needed for establishing a communication link between two far-end modems. These procedures are accomplished using

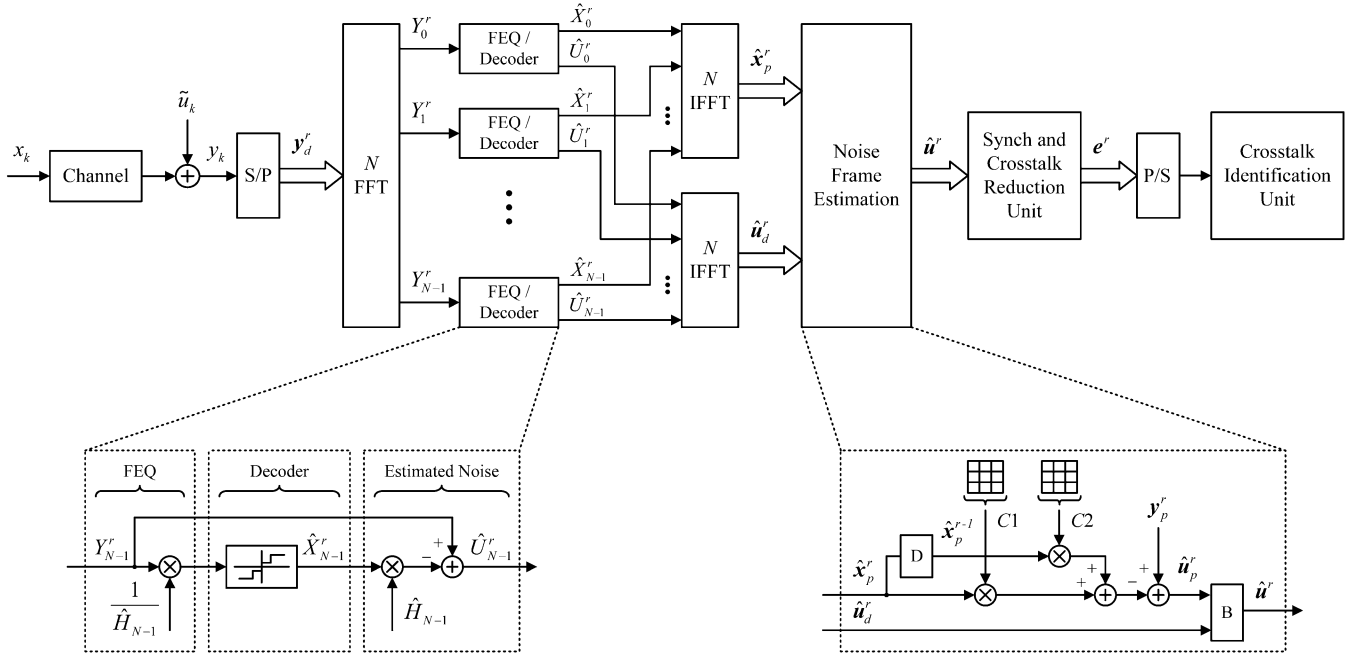


Fig. 4. General block diagram for noise frame estimation.

handshaking sequences that enable the activation of the DSL link and determine certain attributes of the communication channel. Based on these attributes, both modems establish certain transmission characteristics that maximize the system throughput and reliability.

According to Recommendation G.992.1 [8], the signal-to-noise ratio (SNR) estimation is based on channel measurements of a specific wide-band pseudo-random signal (PRD), sent by the far-end transmitter at high power level. As a result, the training signals of a new activated line generate additional FEXT crosstalk noise to the receivers of all active lines. Since the receiver of any active line knows the characteristics of the PRD signal, it can exploit that knowledge in order to detect the activation of another line and to estimate the respective crosstalk coupling function. Therefore, the crosstalk identification process constitutes of the following major steps:

- 1) detection of the existence of a new ADSL training sequence;
- 2) synchronization on the PRD sequence frame;
- 3) estimation of the crosstalk coupling function.

The signal received by the CPE modem of an active line is corrupted by noise that consists of AWGN and FEXT components. In conditions of error-free transmission, this noise can be estimated using the differences between the input and the output at the decoder stage. In case of erroneous decoding, the noise estimation is affected by the decoding errors, although in this case, the increased BER may force the modems to re-execute channel training. In the rest of this paper, we consider the case of error-free decoding.

### III. TRAINING DETECTION AND TIMING SYNCHRONIZATION

This section describes the process for extracting the crosstalk-related information in a disturbed line and the synchronization

of the disturbed modem to the disturber's timing. Fig. 4 shows a general model of an active DMT receiver. Modeling the channel as a finite impulse response (FIR) filter with  $L_{ch}$  real taps, the received time-domain sequence is given by

$$y_k = h_k * x_k + \tilde{u}_k = \sum_{i=0}^{L_{ch}-1} h_i x_{k-i} + \tilde{u}_k \quad (4)$$

where  $x_k$  is the transmitted signal,  $h_k$  is the channel impulse response, and  $\tilde{u}_k$  represents the noise experienced at the receiver, which consists of AWGN and crosstalk noise. In DMT systems, the data are transmitted using  $N + \nu$  size blocks, where  $\nu$  ( $\nu \geq L_{ch} - 1$ ) is the size of the cyclic prefix that is added in order to avoid intersymbol interference (ISI). We choose  $\nu = L_{ch} - 1$  in order to minimize the data overhead. Then, denoting as  $x_k^r$  the samples transmitted at block  $r$ , for  $k = -\nu, \dots, -1, 0, \dots, N-1$  and as  $x_{-i} = x_{N-i}$  the cyclic prefix, for  $i = 1, \dots, \nu$ , we use (4) to form the following set of  $N + \nu$  equations:

$$\begin{aligned} y_{-\nu}^r &= h_0 x_{-\nu}^r + \dots + h_\nu x_{N-\nu}^{r-1} + \tilde{u}_{-\nu}^r \\ &\vdots \\ y_{-1}^r &= h_0 x_{-1}^r + \dots + h_\nu x_{N-1}^{r-1} + \tilde{u}_{-1}^r \\ y_0^r &= h_0 x_0^r + \dots + h_\nu x_{-\nu}^r + \tilde{u}_0^r \\ &\vdots \\ y_{N-1}^r &= h_0 x_{N-1}^r + \dots + h_\nu x_{N-\nu-1}^r + \tilde{u}_{N-1}^r \end{aligned} \quad (5)$$

The first  $\nu$  equations determine the portion of the received block  $r$ , that is not used at the decoding process. These samples contain the ISI interference from the previous block. The last  $N$  equations determine the useful samples processed by the receiver in order to extract the transmitted information.

### A. Noise Frame Estimation

Using matrix notation, the useful portion of the received sequence can be written as

$$\mathbf{y}_d^r = C\mathbf{x}_d^r + \tilde{\mathbf{u}}_d^r \quad (6)$$

where  $\mathbf{y}_d^r = [y_{N-1}^r, \dots, y_0^r]^T$ ,  $\mathbf{x}_d^r = [x_{N-1}^r, \dots, x_0^r]^T$ ,  $\tilde{\mathbf{u}}_d^r = [\tilde{u}_{N-1}^r, \dots, \tilde{u}_0^r]^T$ ,  $C$  is the channel response matrix and the subscript  $d$  is used to denote the useful data part. Given a cyclic prefix, the channel response matrix is circulant and can always be decomposed [14] as

$$C = Q^* \Lambda Q \quad (7)$$

where  $Q$  is the fast Fourier transform (FFT) matrix and  $\Lambda$  is a diagonal matrix whose diagonal elements correspond to the channel frequency response. The block  $\mathbf{y}_d^r$  is provided to the receiver's FFT stage and the complex output  $\mathbf{Y}_d^r$  is given by

$$\mathbf{Y}_d^r = Q\mathbf{y}_d^r = QC\mathbf{x}_d^r + Q\tilde{\mathbf{u}}_d^r = \Lambda\mathbf{X}_d^r + \tilde{\mathbf{U}}_d^r \quad (8)$$

where  $\mathbf{X}_d^r = Q\mathbf{x}_d^r$  is the  $N$ -points FFT block of the useful transmitted samples and  $\tilde{\mathbf{U}}_d^r = Q\tilde{\mathbf{u}}_d^r$ . Note that the lower half of  $\mathbf{X}_d^r$ , from 0 to  $N/2$ , corresponds to the transmitted subsymbol sequence.

The signal is passed to the frequency domain equalizer (FEQ), for attenuation and phase adjustment at each carrier, and then the slicer/decoder performs an estimation of the transmitted subsymbols sequence. A simple one-tap equalizer is used for multiplying each input subsymbol,  $Y_j$  for  $j = 1, \dots, N$ , with the inverse estimated frequency response  $\hat{H}_j$  of the corresponding subchannel, obtained during transmitter training. Assuming no decoding errors  $\hat{X}_j = X_j$  and perfect estimation of the primary channel,  $\hat{H}_j = H_j$ , the noise estimate is given by

$$\hat{\mathbf{U}}_d^r = \mathbf{Y}_d^r - \Lambda\hat{\mathbf{X}}_d^r. \quad (9)$$

If we perform inverse fast Fourier transform (IFFT) on  $\hat{\mathbf{U}}_d^r$ , we get an estimation of the time domain noise samples that correspond to the useful portion of the received block

$$\hat{\mathbf{u}}_d^r = Q^*\hat{\mathbf{U}}_d^r = \tilde{\mathbf{u}}_d^r. \quad (10)$$

The process described previously can be used to estimate the noise samples  $\hat{u}_k^r$  for  $k = 0, \dots, N-1$  at block  $r$ . Now we are interested in estimating the noise samples for  $k = -\nu, \dots, -1$ .

Observing the first  $\nu$  equations of set (5), we note that the received sequence depends on samples transmitted during the current block,  $x_k^r$  for  $k = -\nu, \dots, -1$ , and on samples transmitted during the previous block,  $x_k^{r-1}$ , for  $k = N-\nu, \dots, N-1$ . In particular, both subsets correspond to the cyclic prefix parts added to the two blocks and can be obtained from the decoded subsymbols  $\hat{\mathbf{X}}_d^r$  and  $\hat{\mathbf{X}}_d^{r-1}$  using IFFT. Using the cyclic prefix definition, we can write the first  $\nu$  equations of (5) in matrix notation as

$$\mathbf{y}_p^r = [C1 \quad C2] \begin{bmatrix} \mathbf{x}_p^r \\ \mathbf{x}_p^{r-1} \end{bmatrix} + \tilde{\mathbf{u}}_p^r \quad (11)$$

where  $\mathbf{y}_p^r = [y_{-1}^r, \dots, y_{-\nu}^r]^T$ ,  $\mathbf{x}_p^r = [x_{N-1}^r, \dots, x_{N-\nu}^r]^T$ ,  $\mathbf{x}_p^{r-1} = [x_{N-1}^{r-1}, \dots, x_{N-\nu}^{r-1}]^T$ ,  $\tilde{\mathbf{u}}_p^r = [\tilde{u}_{-1}^r, \dots, \tilde{u}_{-\nu}^r]^T$ , and the subscript  $p$  is used to denote the cyclic prefix data part. The channel matrices  $C1$  and  $C2$  are defined as

$$C1 = \begin{bmatrix} h_0 & h_1 & \cdots & h_{\nu-1} \\ 0 & h_0 & \cdots & h_{\nu-2} \\ \vdots & \vdots & \ddots & \vdots \\ 0 & 0 & \cdots & h_0 \end{bmatrix} \quad (12)$$

$$C2 = \begin{bmatrix} h_\nu & 0 & \cdots & 0 \\ h_{\nu-1} & h_\nu & \cdots & 0 \\ \vdots & \vdots & \ddots & \vdots \\ h_1 & h_2 & \cdots & h_\nu \end{bmatrix}. \quad (13)$$

From (11) we can get an estimation of the noise samples  $\hat{u}_k^r$  for  $k = -\nu, \dots, -1$

$$\hat{\mathbf{u}}_p^r = \mathbf{y}_p^r - [C1 \quad C2] \begin{bmatrix} \mathbf{x}_p^r \\ \mathbf{x}_p^{r-1} \end{bmatrix} = \tilde{\mathbf{u}}_p^r. \quad (14)$$

The concatenation of the noise values, determined in (10) and (14), provides a complete estimate of noise at block  $r$

$$\hat{\mathbf{u}}^r = [\hat{\mathbf{u}}_d^r \quad \hat{\mathbf{u}}_p^r]^T. \quad (15)$$

This noise signal consists of AWGN, FEXT crosstalk from all active lines, and the FEXT component of the new activated line, with the latter being the useful signal of the crosstalk identification algorithm and is denoted as  $\mathbf{c}^r$ . It is obvious that due to the nature of the crosstalk coupling function, the useful signal has very low SNR.

At the next step, we have to decrease the effect of the crosstalk noise introduced by the active lines. This can be achieved at each CPE modem, since the CO informs all CPE downstream receivers about the bit-loading decisions and the power level distributions of all active lines. Moreover, each CPE modem knows the crosstalk coupling functions between its own line and the other active lines, from estimations performed as described in Section V. Using a procedure similar to the one described previously, the effect of the crosstalk noise introduced by the active lines is partially cancelled and the remaining noise, denoted as  $\mathbf{c}_{\text{rem}}^r$ , along with the AWGN noise  $\mathbf{n}^r$ , determine the useful signal's SNR. Therefore, the input signal,  $\mathbf{e}^r$ , to the crosstalk identification method is given by

$$\mathbf{e}^r = \mathbf{c}^r + (\mathbf{n}^r + \mathbf{c}_{\text{rem}}^r). \quad (16)$$

### B. ADSL Training Sequence Detection

Detection of the disturber's training sequence embedded in (15) is similar to the detection of types of signals transmitted during the ADSL initialization process [8]. In particular, initial detection can be obtained using a narrow bandpass filter in order to capture the transmission of pilot tones sent at specific subchannels. A second detection stage can be performed by a matched filter used to capture the transmission of the specific periodic patterns defined for ADSL systems. Both pilot tones and periodic patterns are transmitted over a large number of symbols during initialization and early enough before the transmission of the PRD for channel identification.

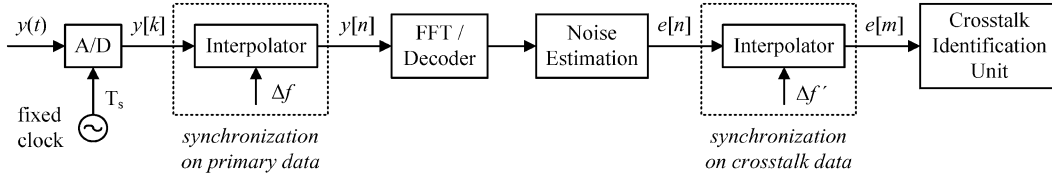


Fig. 5. General block diagram of synchronization units.

### C. Timing Synchronization

In DMT transmission systems we distinguish two types of synchronization: *sample synchronization* and *symbol synchronization* [15]. The first type guarantees frequency alignment between the receiver's and transmitter's sampling clocks, while the second type determines the boundaries of each DMT symbol in the received sample sequence, i.e., the  $N + \nu$  samples that belong to the same symbol.

In our system model, we define as  $f_s$  the sampling frequency of the receiver in the line of interest, called also primary line, and assume perfect synchronization with the far-end transmitter. If we define a sampling frequency difference between the transmitter of the disturber line and the receiver of the primary line, this difference is embedded in the noise signal of (16). A second timing recovery unit is now responsible for synchronization on the crosstalk data stream. An all-digital timing correction scheme is presented in [16]. Fig. 5 shows a general block diagram of the primary line receiver, where the two different synchronization stages are presented.

The analysis of the interpolator's structure and the synchronization method used at the crosstalk identification unit is out of the scope of this paper. In order to include the effect of the timing recovery process, a residual frequency error  $\Delta f'$  is assumed at the recovered noise signal and a fractional error  $\varepsilon = \Delta f' / f_s$  is defined. For ADSL systems the error  $\varepsilon$  is expected to be no more than  $\pm 100$  ppm ( $10^{-4}$ ) [17]. The performance of the crosstalk identification method is analyzed in the next section for different values of this frequency fractional error.

Regarding symbol synchronization, a similar approach is used as in the normal channel training sequence. Symbol synchronization exploits the periodicity of the incoming data frame, in order to estimate its boundaries. When a periodic sequence is received, its periodicity is determined by the length of the sequence. In the case of nonperiodic DMT frames, either known or random, the periodicity is embedded in the cyclic prefix added in the useful data. In [18], a periodicity metric based on correlation of the incoming data with a delayed version is presented. During line training, a periodic pattern, named *Reverb*, is transmitted for a large number of symbols before starting the transmission of the PRD for channel estimation. In our model we assume frame synchronization on the recovered noise signal so that the receiver is able to identify the start of the PRD sequence.

## IV. CROSSTALK IDENTIFICATION

The crosstalk function is identified using a least-squares (LS) estimator. We model the crosstalk coupling function as an FIR filter of size  $L_{cr}$  and let  $K$  denote the number of samples used

for estimation. Note that the estimated crosstalk impulse response is the aggregated crosstalk and receiver's input filter response. The solution to the LS problem is given [19] by

$$\hat{\mathbf{h}} = (T^*T)^{-1}T^*\mathbf{e} \quad (17)$$

where  $\hat{\mathbf{h}}$  is the unbiased estimation of the crosstalk impulse response vector of size  $L_{cr}$ ,  $\mathbf{e}$  is the input noise vector of size  $K$ , and  $T$  is the Toeplitz matrix of the known PRD sequence with size  $K \times L_{cr}$ . Note that the noise vector  $\mathbf{e}$  is generated over a duration of  $K$  samples, as described in (16). Let  $\mathbf{h} = [h_0, h_1, \dots, h_{L_{cr}-1}]^T$  and  $\hat{\mathbf{h}} = [\hat{h}_0, \hat{h}_1, \dots, \hat{h}_{L_{cr}-1}]^T$  denote the actual and the estimated crosstalk vectors. In order to evaluate the estimation accuracy we use the following metric:

$$M = \frac{\|\mathbf{h}\|^2}{E[\|\Delta\mathbf{h}\|^2]} \quad (18)$$

where  $\Delta\mathbf{h} = \hat{\mathbf{h}} - \mathbf{h}$  is the estimation error vector and  $\|\cdot\|$  denotes the norm of the vector. The above metric represents the signal-to-estimation error ratio.

In the rest of this section, we present simulation results that demonstrate the accuracy of the method described previously for estimating the crosstalk coupling function. The initial performance results study the effect of the synchronization error  $\varepsilon$  and the number of samples  $K$  of the LS method under the same noise conditions, while at the next subsection we study the effect of the total noise level on the method's accuracy.

### A. Implementation Parameters Effect

In our analysis, we considered subscriber loops of 9 kft 26 AWG that correspond to the standard #6 CSA test-loop [8]. According to (1), the FEXT noise is directly proportional to the coupling path length, and the test-loop considered represents a typical case with remarkable attenuation.

Fig. 6 shows the estimated coupling function relative to the ideal crosstalk coupling function, for  $-140$  dBm/Hz AWGN and 10 000 samples, under different synchronization errors  $\varepsilon$ . We observe that the higher the frequency fractional error, the greater is the variation, especially in subchannels with stronger attenuation. In fact, due to the synchronization error, the observed signal  $\mathbf{e}$  of the LS method corresponds to different time span of the known PRD signal, although the same number of samples is used for both signals. As a result, the method produces an estimate that differs from the original coupling function as  $\varepsilon$  increases. For  $\varepsilon > 10^{-4}$ , the estimated coupling function exhibits significant variations. In Fig. 6 we observe that for  $\varepsilon = 10^{-5}$  and for 10 000 samples, a good approximate of the original crosstalk coupling function is achieved.

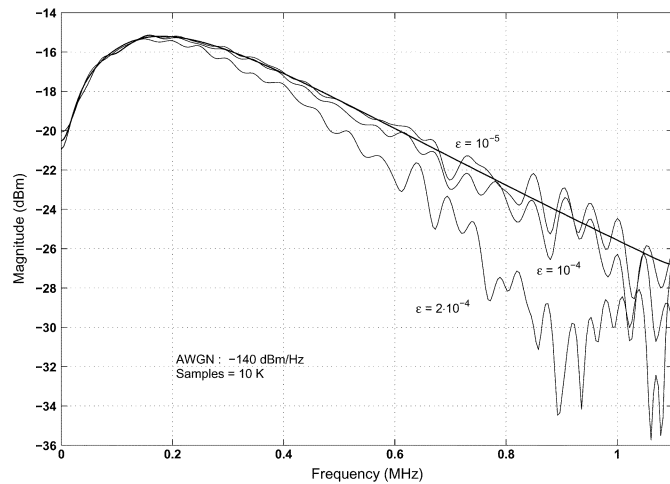


Fig. 6. Dependence of the crosstalk coupling function estimation on the frequency fractional error.

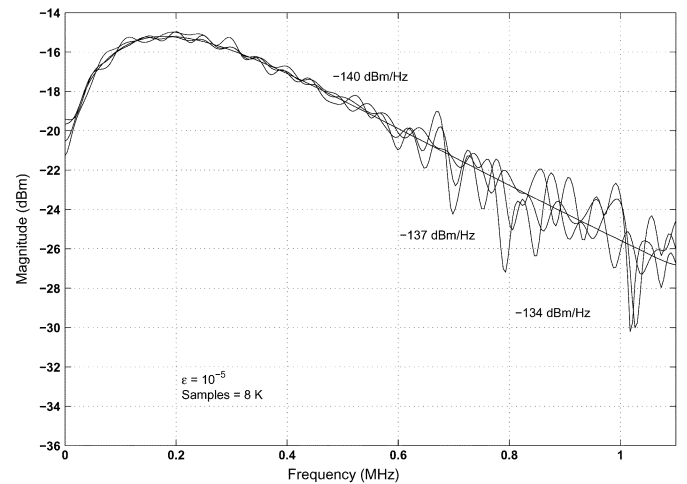


Fig. 8. Dependence of the crosstalk coupling function estimation on the noise level.

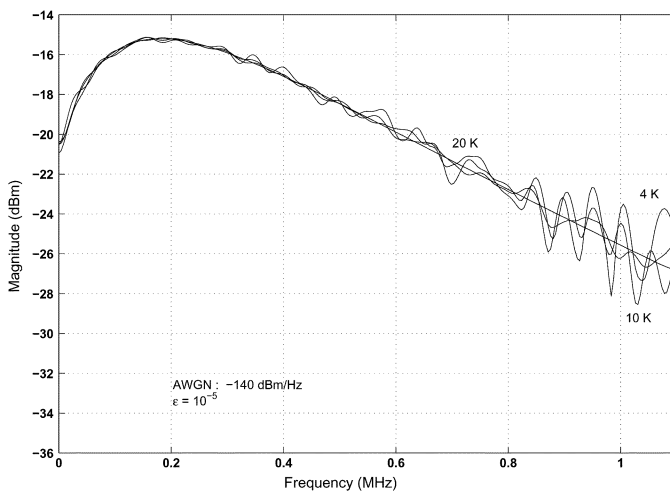


Fig. 7. Dependence of the crosstalk coupling function estimation on the number of samples.

Fig. 7 presents the coupling function estimation for  $-140$  dBm/Hz AWGN and  $\varepsilon = 10^{-5}$ , when different numbers of samples are used. The estimation accuracy also depends on the number of samples used in the LS method. For 4000 samples the estimation exhibits large variation, while for 20 000 samples the variation decreases significantly. For small values of  $\varepsilon$ , increasing the number of samples results to better coupling function estimation, as expected. However, as the value of  $\varepsilon$  increases, the estimation of the coupling function may become less accurate when more samples are used, since a larger time span difference exists between the input and the known PRD signals.

### B. Noise Level Effect

Fig. 8 presents the estimated coupling function, under different levels of system noise, for  $\varepsilon = 10^{-5}$  and 8000 samples. We observe that the case of  $-140$  dBm/Hz produces intermediate estimation results compared to the plots of Fig. 7 for 4000 and 10 000 samples. The other two plots of Fig. 8 correspond to 3 and 6 dB higher noise levels respectively. It is obvious that for a given number of samples, the variation increases with the

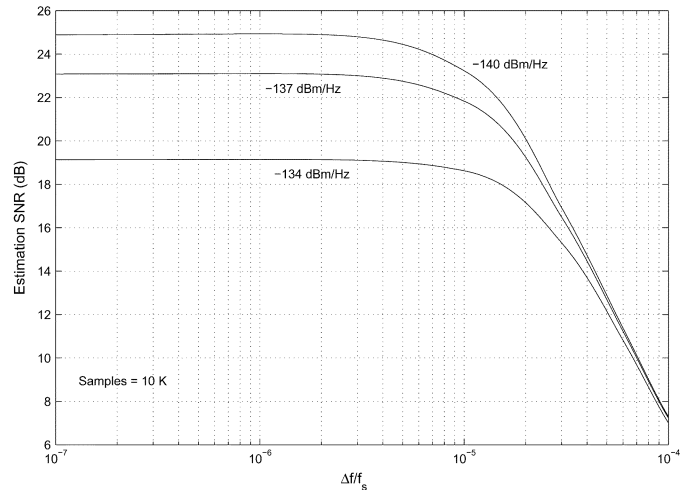


Fig. 9. Estimation SNR as a function of the frequency fractional error  $\varepsilon = \Delta f' / f_s$ .

noise level. In this case using more samples would improve the estimation accuracy.

The effect of the system noise and synchronization error can be further examined using the metric of (18), which represents the SNR of the estimation process. Fig. 9 shows this metric as a function of the frequency fractional error and for different noise levels. The number of samples used for the estimation is 10 000. This figure shows that for small values of the synchronization error, the metric remains constant and depends only on the noise level. When the synchronization error exceeds a specific value, the error introduced due to the frequency offset becomes dominant. Small frequency fractional errors  $\varepsilon$  produce a quite similar output sequence at the second synchronization unit of Fig. 5, so that the estimation error vector  $\Delta \mathbf{h}$  changes slightly. Moreover, as also indicated in Fig. 8, for constant number of samples, the higher the noise level, the less accurate is the approximation of the crosstalk coupling function, and the estimation SNR decreases. When the synchronization error exceeds the value of  $10^{-4}$ , no reliable results can be obtained using the LS estimation method.

We define the method's estimation error (in percentage) as the inverse of the metric of (18). Fig. 10 shows how the estimation

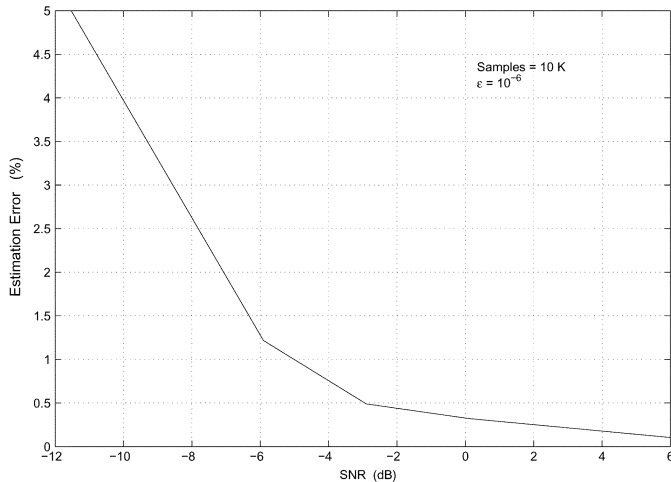


Fig. 10. Crosstalk identification error as a function of SNR.

error depends on the SNR of the desired signal at the input of the crosstalk identification unit when the synchronization error remains low. The SNR is defined as the ratio of the power of the crosstalk injected signal to the power of the total remaining noise in the primary line. This figure demonstrates that, for a given level of total remaining noise in the primary line, the use of the LS method, in terms of the lower possible limit, depends on the magnitude of the crosstalk coupling function, even if no synchronization error is encountered.

## V. SIGNALING PROTOCOL AND CROSSTALK IDENTIFICATION PROCEDURES

During data transmission, the two modems of a DSL line (called the ATU-C and the ATU-R modem) use specific fields of each superframe in order to exchange physical layer operational information. The ATU-C modem is directly attached to the CO, exchanges operational and maintenance information with the CO management unit and supports the exchange of information between the CO and the ATU-R modem. Based on the previously described crosstalk identification method, in this section we explain how the CO can coordinate the operation of the various DSL lines in order to perform identification of the crosstalk coupling function between any pair of DSL lines.

We define as  $H_{i,j}$  the crosstalk coupling function from the disturber line  $i$  to the disturbed line  $j$ . If  $k$  lines are already active in the binder, a new line is activated and following the procedures described in Section IV during the signaling phases of line  $k+1$ , the crosstalk coupling functions  $H_{k+1,1}, \dots, H_{k+1,k}$  are determined simultaneously at the rest  $k$  ATU-R modems. In order to determine the crosstalk coupling functions  $H_{1,k+1}, \dots, H_{k,k+1}$ , the signaling phases at lines  $1, \dots, k$  have to be re-executed under the supervision of the CO. This is done progressively, so that only one line at a time re-executes signaling, while the other, not yet re-initialized lines, remain inactive temporarily.

At each step, the CO is updated with the crosstalk estimation performed at the last activated line and this information, along with the loading algorithm results, is forwarded to all active modems. This procedure continues until all  $H_{i,j}$  crosstalk coupling functions have been determined.

As an example, we consider the case of a bundle of three ADSL lines, named  $A$ ,  $B$ , and  $C$ . Line  $A$  is initially activated and using the channel training procedure, its two modems determine the transfer function of line  $A$ . When line  $B$  is activated, the downstream receiver of line  $A$  is able to determine the crosstalk coupling function  $H_{B,A}$ , based on the analysis described in Section IV. Then the CO forces the modems at line  $A$  to re-execute the initialization phases and therefore, the crosstalk coupling function  $H_{A,B}$  is determined. When line  $C$  is activated, the crosstalk coupling functions  $H_{C,A}$  and  $H_{C,B}$  are determined. Then the CO forces the modems at line  $A$  to re-execute the initialization phases, while the modems of line  $B$  remain inactive temporarily, and the crosstalk coupling function  $H_{A,C}$  is determined. Then, the CO forces the modems at line  $B$  to re-execute the initialization phases and the crosstalk coupling function  $H_{B,C}$  is also determined.

Since the crosstalk functions depend on the physical properties of the binder and do not depend on the exchanged information and the order of activation of the various lines, the above described procedure has to be executed only once in a binder (usually during the installation of the modems in the binder) and the respective information has to be stored in the CO, so that the interruption of the provided services at each line becomes negligible. The information that describes the crosstalk functions between any two lines in a binder can be exploited by a centralized bit-loading algorithm for maximizing the binder's performance.

## VI. CONCLUSION

This paper described a crosstalk identification method that is based on measurements performed during transceiver training of ADSL modems operating in the same binder. Since the crosstalk signal of interest is several dBs below the data-related signal transmitted on the same line, the signal has to be improved by removing the components that are not useful for the identification process. In this work, we proposed a procedure for removing the decoded data and the crosstalk noise injected by other disturbers and for synchronizing a remote modem to the crosstalker's timing. Based on this approach, the SNR of the signal of interest is improved considerably, making the estimation of the crosstalk coupling function feasible. In order to improve the system noise tolerance, it is important to use a bit-loading mechanism that maximizes the noise margin under the worst case crosstalk conditions. A weighted margin maximization bit-loading was also proposed that takes into account the FEXT PSD over the ADSL spectrum. As the performance results show, the timing synchronization error at the receiver is crucial to the method's performance and it has to remain below a specific limit. The method's accuracy also depends on the level of the background noise and on the receiver's capability to remove the signals injected by other disturbers with known crosstalk coupling functions. The presented estimation method of the FEXT coupling function can be exploited by a central management unit located at the CO in order to optimize the bit and power distributions of all ADSL lines operating in the same binder.

## REFERENCES

- [1] J. W. Cook *et al.*, "The noise and crosstalk environment for ADSL and VDSL systems," *IEEE Commun. Mag.*, vol. 37, no. 5, pp. 73–78, May 1999.
- [2] *Spectrum Management for Loop Transmission Systems*, Jan. 2001. ANSI Std. T1.417-2001.
- [3] J. M. Cioffi *et al.*, "Proposed scope and mission for dynamic spectrum management," ANSI Contribution T1E1.4/2001-188R4, Greensboro, NC, Nov. 2001.
- [4] K. B. Song *et al.*, "Dynamic spectrum management for next-generation DSL systems," *IEEE Commun. Mag.*, vol. 40, no. 10, pp. 101–109, Oct. 2002.
- [5] K. J. Kerpez *et al.*, "Advanced DSL management," *IEEE Commun. Mag.*, vol. 41, pp. 116–123, Sep. 2003.
- [6] S. Galli, C. Valenti, and K. J. Kerpez, "A frequency-domain approach to crosstalk identification in xDSL systems," *IEEE J. Sel. Areas Commun.*, vol. 19, no. 8, pp. 1497–1506, Aug. 2001.
- [7] C. Zeng *et al.*, "Crosstalk identification in xDSL systems," *IEEE J. Sel. Areas Commun.*, vol. 19, no. 8, pp. 1488–1496, Aug. 2001.
- [8] *Asymmetrical Digital Subscriber Line (ADSL) Transceivers*, July 1999. ITU-T Recommendation G.992.1.
- [9] T. Starr, J. M. Cioffi, and P. J. Silverman, Eds., *Understanding Digital Subscriber Line Technology*. Upper Saddle River, NJ: Prentice-Hall, 1999.
- [10] J. Lee, R. V. Sonalkar, and J. M. Cioffi, "Multi-user discrete bit loading for DMT-based DSL systems," in *IEEE Globecom'02*, vol. 2, Nov. 2002, pp. 1259–1263.
- [11] J. M. Cioffi, "A Multicarrier Primer," ANSI Contribution T1E1.4/91-157, Clearfield, FL, Nov. 1991.
- [12] B. S. Krongold, K. Ramchandran, and D. L. Jones, "Computationally efficient optimal power allocation algorithms for multicarrier communication systems," *IEEE Trans. Commun.*, vol. 48, no. 1, pp. 23–27, Jan. 2000.
- [13] R. V. Sonalkar and R. R. Shively, "An efficient bit-loading algorithm for DMT applications," *IEEE Comm. Letters*, vol. 4, no. 4, pp. 80–82, Mar. 2000.
- [14] C. Zeng and J. M. Cioffi, "Near-end crosstalk mitigation in ADSL systems," *IEEE J. Sel. Areas Commun.*, vol. 20, no. 6, pp. 949–958, Jun. 2002.
- [15] T. Pollet and M. Peeters, "Synchronization with DMT modulation," *IEEE Commun. Mag.*, vol. 37, no. 4, pp. 80–86, Apr. 1999.
- [16] E. Martos-Naya *et al.*, "Optimized interpolator filters for timing error correction in DMT systems for xDSL applications," *IEEE J. Sel. Areas Commun.*, vol. 19, no. 12, pp. 2477–2485, Dec. 2001.
- [17] N. P. Sands and K. S. Jacobsen, "Pilotless timing recovery for baseband multicarrier modulation," *IEEE J. Sel. Areas Commun.*, vol. 20, no. 6, pp. 1047–1054, Jun. 2002.
- [18] P. R. Chevillat, D. Maiwald, and G. Ungerboeck, "Rapid training of a voiceband data-modem receiver employing an equalizer with fractional-T spaced coefficients," *IEEE Trans. Commun.*, vol. 35, no. 9, pp. 869–876, Sep. 1987.
- [19] N. Benvenuto and G. Cherubini, Eds., *Algorithms for Communications Systems and their Applications*. Chichester, U.K.: Wiley, 2002.



**Nikolaos Papandreou** (M'03) was born in Athens, Greece, in 1975. He received the diploma and the Ph.D. degree in electrical engineering and computers technology from the University of Patras, Patras, Greece, in 1998 and 2004, respectively.

Since 1998, he has been a Research Engineer at the Department of Electrical Engineering and Computers Technology, University of Patras, participating in national and European research and development projects in the fields of data communications and embedded systems. In 2000, he also joined the Research Academic Computer Technology Institute, Greece. His research interests are in the areas of communication theory, coding, and signal processing for data transmission with an emphasis in multicarrier systems.

Dr. Papandreou is a member of the Technical Chamber of Greece.



**Theodore Antonakopoulos** (M'88–SM'99) was born in Patras, Greece in 1962. He received the Electrical Engineering Diploma degree and the Ph.D. degree from the Department of Electrical Engineering at the University of Patras in 1985 and 1989, respectively. In September 1985, he joined the Department of Electrical Engineering, University of Patras, participating in various R&D projects for the Greek Government and the European Union, initially as a research staff member and subsequently as the Senior Researcher of the Communications

and Embedded Systems Group. Since 1991, he has been on the faculty of the Electrical Engineering Department, University of Patras, where he is currently an Associate Professor. His research interests are in the areas of data communication networks, LANs and wireless networks, with emphasis on performance analysis, efficient hardware implementation, and rapid prototyping. He has more than 100 publications in the above areas and is actively participating in several R&D projects of European industries. Dr. Antonakopoulos is a Senior member of the IEEE, and is a member of the Technical Chamber of Greece.